JOURNAL OF COMPUTATIONAL PHYSICS **146,** 726–746 (1998)
ARTICLE NO. CP986081

Numerical Solution of Fisher's Equation Using a Moving Mesh Method

Y. Qiu[1] and D. M. Sloan[2]

Department of Mathematics, University of Strathclyde, Glasgow G1 1XH, Scotland
E-mail: y.qiu@strath.ac.uk, d.sloan@strath.ac.uk

Received March 3, 1998; revised August 4, 1998

The paper investigates the viability of using moving mesh methods to simulate travelling wave solutions of Fisher's equation. Results are presented that illustrate the weaknesses in moving mesh methods based on equidistribution of some popular monitor functions. It is shown that knowledge of the differential equation and the travelling wave solution may be used to construct a monitor function that yields accurate results with suitably chosen moving mesh methods. A comparison is made between a moving mesh partial differential equation and a moving mesh differential-algebraic equation for the evolution in time. © 1998 Academic Press

1. INTRODUCTION

1.1. *Fisher's Equation*

R. A. Fisher [7] introduced a nonlinear parabolic partial differential equation on an infinite spatial domain to model the simultaneous growth and spread of a dominant gene. This equation—now popularly known as Fisher's equation—may be written for one space dimension as

$$\frac{\partial u}{\partial t} = \frac{\partial^2 u}{\partial x^2} + u(1-u), \quad x \in (-\infty, \infty),\ t > 0, \tag{1.1}$$

$$\lim_{x \to -\infty} u(x,t) = 1, \qquad \lim_{x \to \infty} u(x,t) = 0, \tag{1.2}$$

$$u(x,0) = u_0(x), \qquad x \in (-\infty, \infty). \tag{1.3}$$

If $u_0(x) \in [0,1]$ on $\mathbb{R}$ it has been shown by Kolmogorov *et al.* [17] that for every $c \geq 2$ there exists a travelling wave solution to (1.1)–(1.3) of wave speed c; that is, a solution of the form $u(x,t) = V_c(x - ct)$ for some function V_c of the scalar variable $\xi = x - ct$. Each of

[1] Supported by the University of Strathclyde and by the ORS Awards Scheme.

[2] Corresponding author.

0021-9991/98 $25.00

these solutions satisfies $V_c(\xi) \in [0, 1]$ for all ξ, and no such solutions exist for $c \in [0, 2)$. If $u_0(x)$ is a positive function that satisfies the boundary conditions (1.2) on $\mathbb{R}$, and if

$$u_0(x) \sim e^{-\beta x} \quad \text{as } x \to \infty, \tag{1.4}$$

then, as $t \to \infty$, u will evolve to a travelling wave with speed $c(\beta)$ [11], where

$$c(\beta) = \begin{cases} \beta + \frac{1}{\beta}, & \beta \leq 1, \\ 2, & \beta \geq 1. \end{cases} \tag{1.5}$$

The propagation speed of the wave has the minimum value $c = 2$ only if the initial distribution amplitude falls off sufficiently rapidly with x as $x \to \infty$; otherwise a speed higher than the minimum can be maintained indefinitely. Note that the speed of the wave is determined by the behaviour of the initial data as $x \to \infty$.

The computational representation of the evolving travelling wave solution to (1.1)–(1.3) is a challenging numerical problem. Numerical schemes may lead to erroneous results if they do not explicitly take into account the delicate solution dependence on the initial distribution behaviour at infinity. To perform a computational solution to (1.1)–(1.3) it is normal to replace the pure Cauchy problem by an initial and boundary value problem on the finite spatial domain $[x_L, x_R]$, with approximate boundary conditions imposed at $x = x_L$ and $x = x_R$. Gazdag and Canosa [8] have produced a numerical solution of (1.1)–(1.3) on a finite domain and they have demonstrated that if boundary conditions of the form (1.2) are imposed at $x = x_L$ and $x = x_R$, the solution evolves towards the travelling wave with minimum speed $c = 2$. They have shown that if the initial condition in $[x_L, x_R]$ is given by a travelling wave profile of speed greater than $c = 2$, the time required to evolve to the minimum wave speed profile is related to the right-hand cutoff point $x = x_R$.

Hagstrom and Keller [11] have shown that travelling wave solutions with speeds greater than $c = 2$ can be accurately represented on a finite domain. The key to their success is the choice of boundary conditions at the cutoff points, particularly at $x = x_R$. An asymptotic representation of the boundary condition is imposed at $x = x_R$, and this condition takes account of the initial data in the discarded region $x > x_R$. A similar approach is used by Hagstrom and Keller [11] to construct an asymptotic boundary condition at left-hand boundary $x = x_L$. It is shown, however, that the solution is much less sensitive to the imposed condition at $x = x_L$, and the authors obtain accurate results using $u(x_L, t) = 1$ and $u_x(x_L, t) = 0$ for $t \geq 0$. It is the initial data in the right tail that determines the wave speed, and it is the right-hand boundary condition that is important. The condition $u(x_R, t) = \text{const}$ leads to good results when the speed of the coordinate system is the same as the speed of the final travelling wave. This speed might not be known in a more complicated problem, and solution in a fixed reference frame with the appropriate asymptotic condition at $x = x_R$ is appropriate.

The stability of the travelling wave and the sensitivity of the solution to the boundary condition ahead of the wave have been discussed by many authors (see, for example, [3, 9–11, 16, 17]). It is readily shown that the equilibrium solutions $u \equiv 0$ and $u \equiv 1$ of Eq. (1.1) are unstable and stable, respectively, to small disturbances. It has been shown (see, for example, [8–10]) that all travelling waves are stable to small perturbations of compact support, but they are unstable to small perturbations of infinite support. We shall comment further on the stability and sensitivity of the travelling wave in Section 4.

1.2. *Objectives*

The first objective in this work is to investigate the viability of moving mesh finite difference methods for the approximate solution of the challenging problem that is outlined in the preceding section. The study was motivated by a comment in Li, Petzold, and Ren [19] to the effect that moving mesh methods are not recommended for reaction–diffusion problems in which the diffusion term is much smaller than the reaction term. They considered a scaled Fisher's equation in the form

$$\frac{\partial u}{\partial t} = \frac{\partial^2 u}{\partial x^2} + \rho u(1-u), \quad x \in (-\infty, \infty), \tag{1.6}$$

where ρ is a (large) positive constant. The initial and boundary conditions are those given by (1.2)–(1.3). It is readily verified that (1.6) has a travelling wave solution satisfying (1.2)–(1.3) of the form

$$u(x,t) = \left(\frac{1}{1+\exp\left(\sqrt{\frac{\rho}{6}}x - \frac{5\rho}{6}t\right)} \right)^2, \tag{1.7}$$

with wave speed $c = 5\sqrt{\rho/6}$. The minimum wave speed of (1.6) is, of course, $2\sqrt{\rho}$, and the work of Gazdag and Canosa [8] indicates that the numerical solution of (1.6) on a finite domain, with initial condition given by (1.7), will evolve to the wave of minimum speed unless great care is taken with the right-hand boundary condition. Li *et al.* [19] avoided the boundary condition problem by solving on the domain [0, 1] with boundary conditions given by the exact solution. They examined the effectiveness of moving mesh methods in simulating the profile accurately and in capturing the correct wave speed. The poor results obtained in the case $\rho = 10^4$ led them to conclude that moving mesh methods were not recommended for this type of situation.

Our aim is to follow the approach of Li *et al.* [19] and to seek improved results using a method based on equidistribution of a monitor function that is constructed from the features of the solution being computed. In adaptive approximation methods it is essential that care be taken in selecting the monitor function for the equidistribution process, as demonstrated in the function approximation problem by Carey and Dinh [4]. We show initially that moving mesh methods based on the familiar arc-length or curvature monitor functions [1, 20, 23] yield inaccurate results. Good numerical solutions that are free of oscillation are then produced using our specially constructed monitor function.

A second objective is to make a comparison between the moving mesh partial differential equation (MMPDE) method proposed by Huang, Ren, and Russell [13] and the moving mesh differential-algebraic equation (MMDAE) method proposed by Mulholland, Qiu, and Sloan [20] for this difficult problem. It emerges that the computed solution is very sensitive to the choice of relaxation parameter, τ, in the MMPDE approach. No such choice is necessary with the MMDAE method. The DAE that is used is a stable, index 1 system [5, 20, 22]. The index 1 property is established in the Appendix for a simple choice of monitor function in the equidistribution process.

2. MOVING MESH METHODS

Moving mesh methods have been used widely during the last few years for solving time-dependent partial differential equations (PDEs). Fairly robust methods have been presented

for problems in one space dimension (see, for example, [6, 13, 20] and references therein), and much is currently being done in developing methods for problems in two space dimensions [15]. These methods move the mesh points as time evolves, with the motion designed to minimise some measure of the computational error. In this work we make use of two moving mesh methods that adapt the mesh to the evolving computational solution by equidistributing some function uniformly over the domain of the problem at specified values of time.

To effect a numerical solution of Eq. (1.6), the equation is recast in terms of independent variables η and t, where η is defined by a one-to-one coordinate transformation of the form

$$x = x(\eta, t). \tag{2.1}$$

This map relates the evenly spaced nodes

$$\eta_i = -1 + \frac{2i}{N}, \quad i = 0, 1, \ldots, N, \tag{2.2}$$

in $[-1, 1]$ to the nodes $\{x_i\}_{i=0}^N$ in $[x_L, x_R]$, where

$$x_L = x_0(t) < x_1(t) < \cdots < x_N(t) = x_R \quad \forall t \geq 0.$$

For moving mesh computations it is convenient to write the differential equation (1.6) in the Lagrangian form [20]

$$\dot{u} - \dot{x}\frac{\partial u}{\partial x} = \frac{\partial^2 u}{\partial x^2} + \rho u(1-u), \tag{2.3}$$

in which $\dot{u}$ and $\dot{x}$ denote derivatives with η held constant. We seek approximations to the time-dependent vectors $\{x_i\}_{i=0}^N$ and $\{u_i\}_{i=0}^N$, where $x_i = x_i(t) = x(\eta_i, t)$ and $u_i = u(x_i, t)$. A semi-discrete version of (2.3) is

$$\dot{u}_i - \dot{x}_i \frac{u_{i+1} - u_{i-1}}{x_{i+1} - x_{i-1}} = \frac{2}{x_{i+1} - x_{i-1}} \left(\frac{u_{i+1} - u_i}{x_{i+1} - x_i} - \frac{u_i - u_{i-1}}{x_i - x_{i-1}} \right) + \rho u_i (1 - u_i) \tag{2.4}$$

for $i = 1, 2, \ldots, N-1$. As stated in the preceding section, the boundary conditions are given by the exact solution (1.7) at $x = x_L$ and $x = x_R$, and this provides the values of u_0 and u_N.

To adapt the mesh to the solution we follow Huang *et al.* [13] in using the equidistribution principle (EP)

$$\int_{x_L}^{x(\eta,t)} M(s, t)\, ds = \eta \int_{x_L}^{x_R} M(s, t)\, ds, \tag{2.5}$$

where M (>0) denotes the monitor function. Differentiation of (2.5) with respect to η gives the differential form of the EP,

$$\frac{\partial}{\partial \eta} \left(M(x(\eta, t), t) \frac{\partial}{\partial \eta} x(\eta, t) \right) = 0, \tag{2.6}$$

and this has been used by Huang *et al.* [13] to derive a set of moving mesh PDEs (MMPDEs). The member of this set that we make use of here is MMPDE6 which is thought to be the most accurate of these [14],

$$\frac{\partial^2 \dot{x}}{\partial \eta^2} = -\frac{1}{\tau}\frac{\partial}{\partial \eta}\left(M\frac{\partial x}{\partial \eta}\right), \tag{2.7}$$

in which τ is a small positive time relaxation parameter in the range $0 < \tau \ll 1$. Using second-order central differences on the grid (2.2) we obtain the semi-discrete mesh equations

$$\dot{x}_{i-1} - 2\dot{x}_i + \dot{x}_{i+1} = -\frac{1}{\tau}[\tilde{M}_{i+1/2}(x_{i+1} - x_i) - \tilde{M}_{i-1/2}(x_i - x_{i-1})] \tag{2.8}$$

for $i = 1, 2, \ldots, N-1$, with

$$x_0(t) = x_L \quad \text{and} \quad x_N(t) = x_R. \tag{2.9}$$

In Eq. (2.8), $\tilde{M}_{i+1/2}$ is a smoothed monitor function defined as in [13, 20] by

$$\tilde{M}^2_{i+1/2} = \frac{\sum_{k=i-p}^{i+p} M^2_{k+1/2}\left(\frac{\gamma}{\gamma+1}\right)^{|k-i|}}{\sum_{k=i-p}^{i+p}\left(\frac{\gamma}{\gamma+1}\right)^{|k-i|}}, \tag{2.10}$$

where $M_{i+1/2}$ approximates the monitor function at $\frac{1}{2}(x_i + x_{i+1})$, γ is a positive real number, and p is a nonnegative integer. In all computations presented in this work we used the fixed values $\gamma = 2$ and $p = 3$. The moving mesh solution of (1.6) by means of MMPDE6 of Huang, Ren, and Russell [13] is given by an approximate time integration of systems (2.4) and (2.8) subject to boundary conditions (2.9), with u_0 and u_N given by the exact solution (1.7) at $x = x_L$ and $x = x_R$.

One of our objectives is to compare the effectiveness of MMPDE6 against that of the moving mesh differential-algebraic equation (MMDAE) approach of Mulholland, Qiu, and Sloan [20]. In the MMDAE method, system (2.8) is replaced by the algebraic equation

$$\tilde{M}_{i+1/2}(x_{i+1} - x_i) - \tilde{M}_{i-1/2}(x_i - x_{i-1}) = 0, \quad i = 1, 2, \ldots, N-1. \tag{2.11}$$

The MMDAE consists of systems (2.4) and (2.11), with boundary conditions as before. The MMDAE imposes the approximate equidistribution condition (2.11) at each instant of time in the time discretisation, whilst the MMPDE contains a parameter τ that represents the time taken to reach equidistribution from some initial state.

The time integrations for MMPDE6 (systems (2.4) and (2.8)) and MMDAE (systems (2.4) and (2.11)) were performed using the stiff ODE/DAE solver DASSL [21] with $ATOL = 10^{-6}$, $RTOL = 10^{-6}$, and $N = 50$. DASSL is an ideal integrator for index 0 and index 1 ODE/DAE systems [2]. The initial values of $\{x_i\}_{i=1}^{N-1}$ were obtained by applying the equidistribution condition (2.11) to the initial data function. Finally, in all of the computations we set $x_L = -0.2$ and $x_R = 0.8$.

3. NUMERICAL RESULTS

3.1. *Arc-Length and Curvature Monitor Functions*

The proper choice of monitor function for a specified problem is still an open question. An analysis of the optimality of meshes and monitor functions for the function approximation problem has been given by Carey and Dinh [4]. Much of the recent work on the solution of PDEs using adaptive methods based on equidistribution have favoured the arc-length monitor function (see, for example, [13, 14, 19, 20]). For this choice, the quantity M in (2.5) takes the form

$$M(x,t) = \sqrt{1+\alpha^2(\partial u/\partial x)^2}, \tag{3.1}$$

and the discrete approximation $M_{i+1/2}$ that appears in (2.10) is

$$M_{i+\frac{1}{2}} = \sqrt{1+\alpha^2\left(\frac{u_{i+1}-u_i}{x_{i+1}-x_i}\right)^2}. \tag{3.2}$$

The user-specified parameter α measures the extent to which the solution slope influences mesh location. In the work presented here α is given the value 2.

Figure 1 shows solutions of Fisher's equation at $t = 5\times 10^{-4}$, computed by means of MMPDE6 and the arc-length monitor function. The objective here is to determine how the choice of the parameter τ in (2.8) influences the quality of the generated mesh and, consequently, the accuracy of the computed solution. The use of a nonzero value of τ has the effect of introducing temporal smoothing in the computed solution [13]. Figures 1a, 1b, and 1c show the computed mesh and solution given by the choices $\tau = 10^{-3}$, 10^{-5}, and 10^{-7}, respectively. Note that at $\tau = 10^{-3}$ and $\tau = 10^{-5}$ the nodes are concentrated at the tail of the travelling wave. For these values of τ, nodal density is very low within the wave and in the region of large curvature at the front of the wave, and, not surprisingly, there is evidence of significant computational error at the wave front. The mesh improves as τ diminishes, and at $\tau = 10^{-7}$ the nodal distribution appears to be much better. It is clear from the displays in Fig. 1 that the computed mesh is sensitive to the choice of τ in the moving mesh PDE.

A further comment should be made on the user-specified parameters τ and α that appear in Eqs. (2.7) and (3.1), respectively. As intimated immediately after the points of first occurrence, τ is a time relaxation parameter and α measures the extent to which the solution slope influences mesh location. The appropriate values of the parameters are related to the scale of the problem. If the independent variables x and t in Eq. (1.6) are re-scaled by means of the transformation

$$t := \rho^{-1}t, \quad x := \rho^{-1/2}x$$

the equation reduces to Eq. (1.1), and the appropriate values of τ and α are altered accordingly. For example, an expanded version of Fig. 1c is obtained if Eq. (1.1) is integrated to $t = 5$ over the spatial domain $-20 < x < 80$, with the arc-length monitor function in MMPDE6. The values of N, *ATOL*, and *RTOL* are identical to those used in producing Fig. 1c, but τ and α take the re-scaled values 10^{-3} ($\rho\times 10^{-7}$) and 200 ($\rho^{1/2}\times 2$), respectively.

The objective in the numerical experiments that are illustrated in Fig. 2 is to determine whether an accurate solution can be computed up to $t = 2.5\times 10^{-3}$ using MMPDE6 with

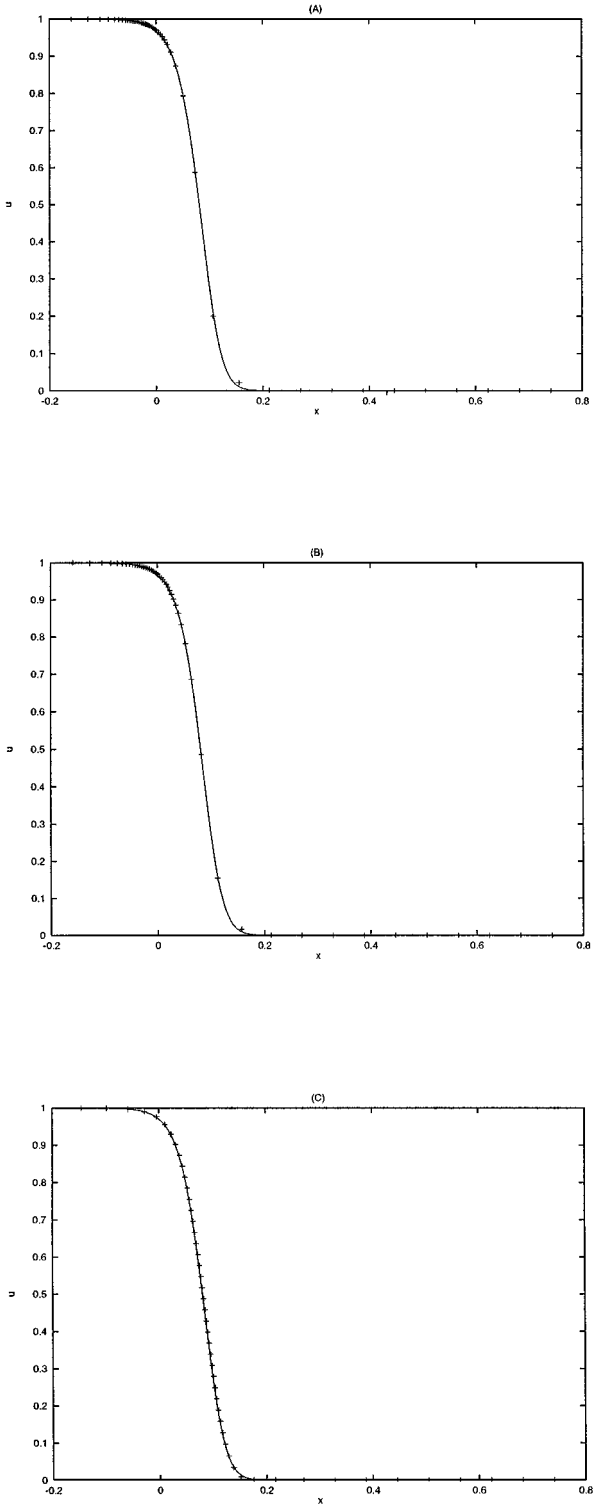

FIG. 1. Numerical solutions of Fisher's equation (1.6) at $t = 5 \times 10^{-4}$, computed by MMPDE6 and the arc-length monitor function: (a) solution with $\tau = 10^{-3}$; (b) solution with $\tau = 10^{-5}$; (c) solution with $\tau = 10^{-7}$.

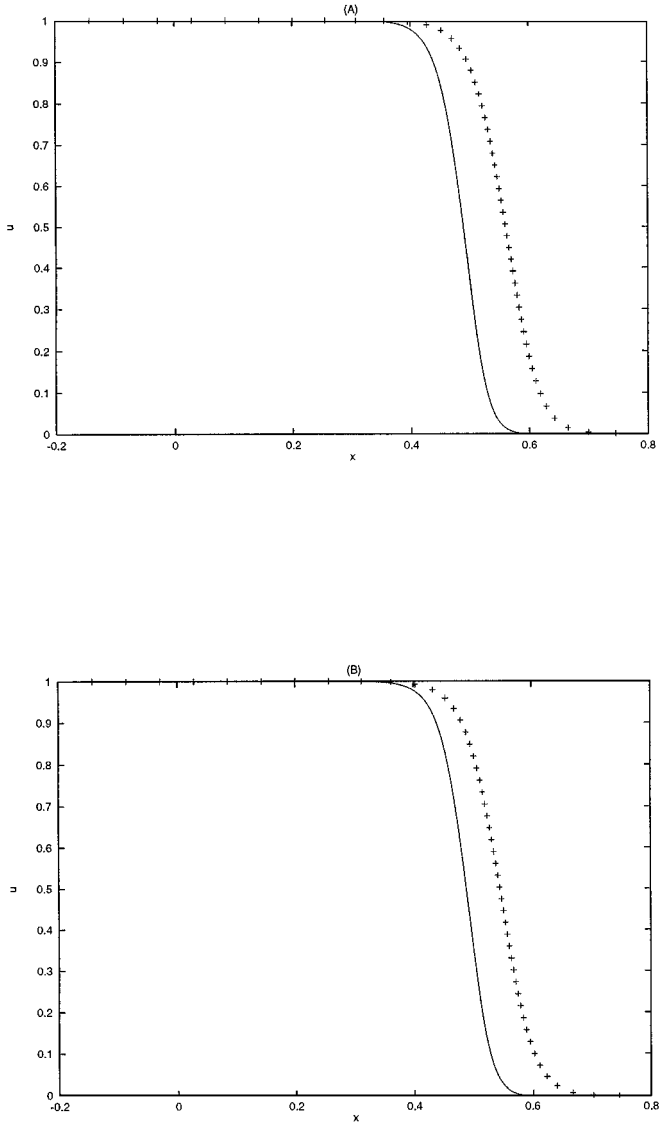

FIG. 2. Numerical solutions of Fisher's equation (1.6) at $t = 2.5 \times 10^{-3}$: (a) solution computed by MMPDE6 and arc-length monitor function with $\tau = 10^{-7}$; (b) by MMDAE and arc-length monitor function. The continuous line gives the exact solution.

$\tau = 10^{-7}$ and an arc-length monitor function. Figure 2a shows that the computed solution for the travelling wave is moving faster than the exact solution; the maximum pointwise error is $O(1)$ at the wave front. The experiment was repeated using MMDAE with arc-length monitor function, and the results are displayed in Fig. 2b. Analogous results have been presented by Li *et al.* [19], and the obvious conclusion is that moving mesh methods based on the arc-length monitor function are not suitable for computational solution of Fisher's equation. It can be seen that the solutions given by MMDAE are similar, in terms of accuracy, to those given by MMPDE6 with $\tau = 10^{-7}$. The proximity of the results given by MMDAE and MMPDE6 with $\tau = 10^{-7}$ is anticipated. We shall see later, however, that

MMPDE6 with $\tau = 10^{-7}$ produces a stiffer system than MMDAE, and this has associated disadvantages in terms of execution time.

Another commonly used monitor function is one in which the first derivative in (3.1) is replaced by the second derivative [1, 23]. This curvature monitor function is given by

$$M(x,t) = \left(1 + \alpha^2 \left(\frac{\partial^2 u}{\partial x^2}\right)^2\right)^{1/4}, \tag{3.3}$$

with

$$M^4_{i+1/2} = 1 + \alpha^2 \left[\frac{1}{x_{i+1} - x_i}\left(\frac{u_{i+2} - u_i}{x_{i+2} - x_i} - \frac{u_{i+1} - u_{i-1}}{x_{i+1} - x_{i-1}}\right)\right]^2. \tag{3.4}$$

At nodes close to x_L and x_R the expression (3.4) has to be modified as has the smoothing operation defined by (2.10). As in the case of arc-length, the parameter α is set to the value 2, and it should be noted that α will be related to the scale of the problem.

Figure 3 shows solutions of Fisher's equation at $t = 5 \times 10^{-4}$, computed by means of MMPDE6 with the curvature monitor function. Solutions given by $\tau = 10^{-3}$, 10^{-5}, and 10^{-7} are displayed in Figs. 3a, 3b, and 3c, respectively. The results show the same weaknesses that were discussed in relation to Fig. 1. The mesh improves as τ diminishes, with a good nodal distribution at $\tau = 10^{-7}$ and overconcentration of nodes behind the wave at the larger values of τ. The computed mesh is sensitive to the choice of τ.

Figure 4 shows the solution computed at the later time, $t = 2.5 \times 10^{-3}$, by means of MMPDE6 with the curvature monitor function and $\tau = 10^{-7}$. In this case the solution is oscillatory at the front of the wave, and again it seems that the monitor function might not be suitable. The MMDAE produces similar results.

3.2. *Modified Monitor Function*

As indicated by Hagstrom and Keller [11] and by Gazdag and Canosa [8], the numerical difficulties that arise in the numerical simulation of the travelling wave for Fisher's equation have their source at the the front of the wave. Hagstrom and Keller [11] have shown that great care is needed in formulation of boundary conditions at $x = x_R$, and Gazdag and Canosa [8] have shown that the computational solution is unstable to roundoff errors introduced at the wave front. Canosa [3] has also shown that all travelling waves are stable to local perturbations, but linearly unstable to perturbations of infinite extent. In Section 4 we use an approach similar to that adopted by Canosa [3] to show that a central difference solution on an even grid of spacing h is stable to local perturbations. If $v_j(t)$ denotes a perturbation about the solution $w_j(t)$, where the subscript j indicates the location $x_j = x_L + jh$, it may be shown that the rate of decay of the perturbation is larger in regions where $w_j \sim 1$ than it is in regions where $|w_j| \ll 1$. This suggests that truncation errors introduced at the front of the wave will be a stronger source of inaccuracy than analogous truncation errors introduced at the rear of the wave. The implication of this in the present context is that a monitor function should be designed to give a high nodal density and, therefore, high accuracy at the wave front where $w_j \sim 0$.

Our objectives in terms of monitor function design have led us to the choice

$$M(x,t) = \left[1 + \alpha^2(1-u)^2 + \beta^2(a-u)^2\left(\frac{\partial^2 u}{\partial x^2}\right)^2\right]^{1/2}, \tag{3.5}$$

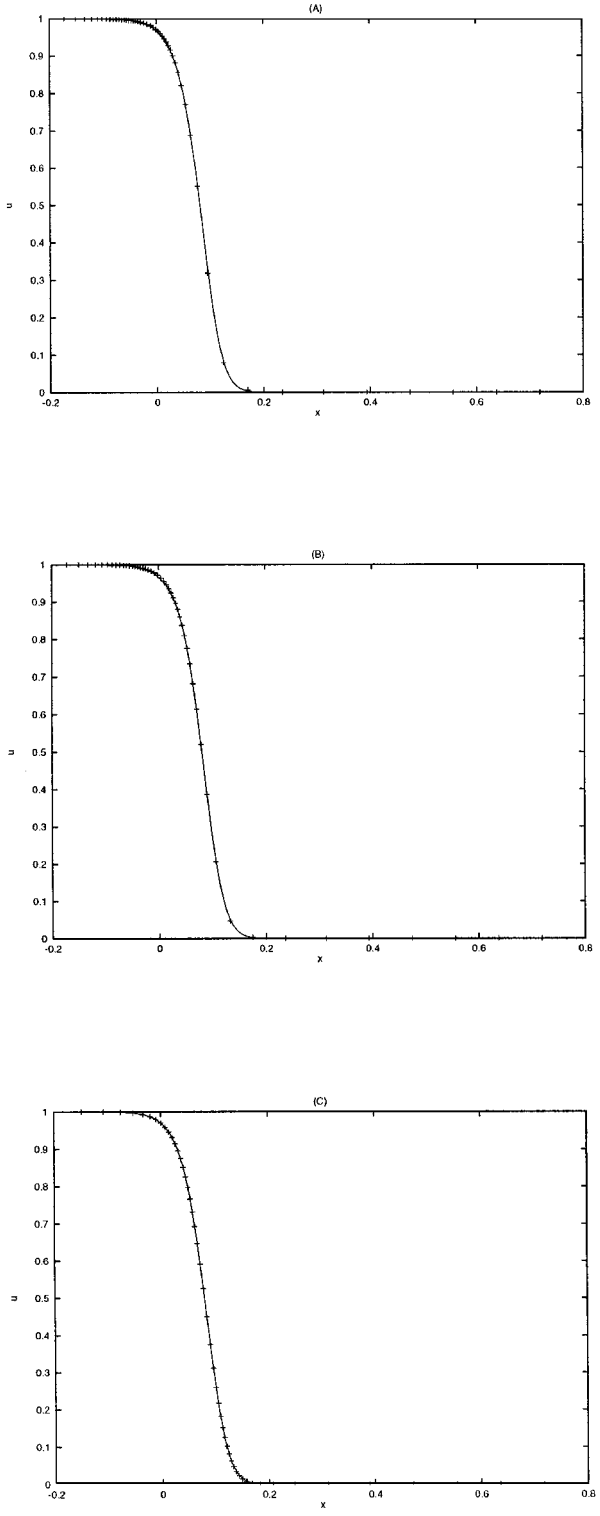

FIG. 3. Numerical solutions of Fisher's equation (1.6) at $t = 5 \times 10^{-4}$, computed by MMPDE6 and curvature monitor function: (a) solution with $\tau = 10^{-3}$; (b) solution with $\tau = 10^{-5}$; (c) solution with $\tau = 10^{-7}$.

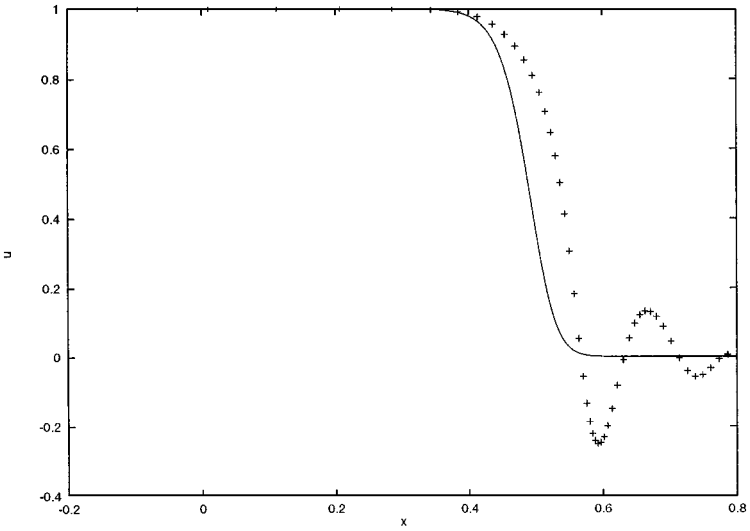

FIG. 4. Numerical solution of Fisher's equation (1.6) at $t = 2.5 \times 10^{-3}$, computed by MMPDE6 and curvature monitor function with $\tau = 10^{-7}$. The continuous line denotes the exact solution.

where, α, β, and a are user-specified parameters. In the computations that are presented in this section we used the values $\alpha = 1.5$, $\beta = 0.1$, and $a = 1.015$. The term $(a - u)^2$ that appears as a multiplying factor with the second spatial derivative takes values close to 1.015^2 and 0.015^2 at the front and at the rear of the wave, respectively. The choice of a value of a close to unity thus ensures that the high curvature region at the front of the wave is given more weight than the corresponding region at the back of the wave. Similarly, the term $(1 - u)^2$ is also designed to give greater weight at the wave front, and it follows that M is larger at the leading high curvature region than it is at the trailing high curvature region. This has the effect of increasing the nodal density at the front relative to that at the back. For this choice of monitor function the ideal values of α and β will depend on the scale of the problem.

Figure 5 shows solutions of Fisher's equation at several values of t, computed by means of MMDAE and the monitor function (3.5). Note the high nodal density at the wave front and the high accuracy up to time $t = 2.5 \times 10^{-3}$. At this time the maximum pointwise error is 9.25×10^{-3}, whereas the corresponding error using the arc-length monitor function is $O(1)$.

The objective in the numerical experiments that are illustrated in Fig. 6 is to determine the influence of the choice of τ on the accuracy achieved by MMPDE6. The displays in Figs. 6a, 6b, and 6c show the solutions produced by MMPDE6 and monitor function (3.5) with $\tau = 10^{-3}$, 10^{-5}, and 10^{-7}, respectively. With $\tau = 10^{-3}$ and $\tau = 10^{-5}$ the region of high nodal density moves at a speed that is lower than the travelling wave speed and $O(1)$ errors are produced at the wave front. The situation is improved when the relaxation parameter, τ, is reduced to 10^{-7}, but the L_∞ error at $t = 2.5 \times 10^{-3}$ is 4.29×10^{-2}, which is larger than that given by the MMDAE. At $\tau = 10^{-7}$, the error in the solution computed at $t = 2.5 \times 10^{-3}$ is not reduced if N is increased beyond the value $N = 50$. However, a reduction in the value of τ at $N = 50$ gives a reduction in the L_∞ error. Numerical experiments that are described by the authors in [22] demonstrate that MMPDE6 with $\tau = 10^{-7}$ will be a much stiffer system than MMDAE. The execution time for MMDAE is approximately 86% of that for

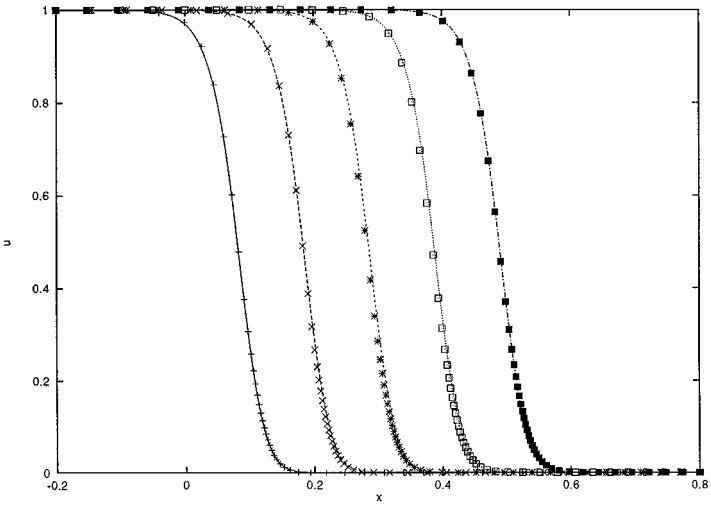

FIG. 5. Numerical solutions of Fisher's equation (1.6) at times $t = 5 \times 10^{-4}$, $t = 1 \times 10^{-3}$, $t = 1.5 \times 10^{-3}$, $t = 2 \times 10^{-3}$, and $t = 2.5 \times 10^{-3}$, computed by MMDAE and the modified monitor function (3.5). The continuous lines represent the exact solutions at the corresponding times.

MMPDE6 in computing the results at $t = 2.5 \times 10^{-3}$ that are displayed in Fig. 5 and Fig. 6c. The comparison of execution times would be even more favourable to MMDAE if we had integrated MMDAE to give an L_∞ error of 4.29×10^{-2} at $t = 2.5 \times 10^{-3}$.

Figure 7 gives the numerical solutions of Fisher's equation at the same values of t as those in Fig. 5, computed by the method of lines on an evenly spaced grid with $N = 50$. The time integration was also performed using DASSL [21] with the same values of *ATOL* and *RTOL* as those used in MMDAE and MMPDE. It shows that the maximum pointwise error is $O(1)$. With the even grid, it is necessary to increase N to 300 to obtain an accuracy at $t = 2.5 \times 10^{-3}$ that is comparable with that of the MMDAE with $N = 50$. The L_∞ error given by the method of lines at $t = 2.5 \times 10^{-3}$ is 9.34×10^{-3} with $N = 300$, and the CPU time is double that of the MMDAE with $N = 50$.

4. STABILITY OF COMPUTED SOLUTION OF (1.6)

The travelling wave with speed c is a solution of the form $u(x, t) = V(x - ct)$, for some function V of the scalar variable $\xi = x - ct$. It is readily seen that V is a solution of the boundary value problem

$$\frac{d^2V}{d\xi^2} + c\frac{dV}{d\xi} + \rho V(1 - V) = 0, \tag{4.1}$$

$$\lim_{\xi \to -\infty} V(\xi) = 1, \quad \lim_{\xi \to \infty} V(\xi) = 0. \tag{4.2}$$

To examine the stability of the travelling wave solution we return to Eq. (1.6) and write this equation in a reference frame that is moving in the positive x direction with speed c. The transformation is effected by casting the equation in terms of independent variables (ξ, t), where $\xi = x - ct$. If $u(x, t) \equiv v(\xi, t)$ then v satisfies the equation

$$\frac{\partial v}{\partial t} = \frac{\partial^2 v}{\partial \xi^2} + c\frac{\partial v}{\partial \xi} + \rho v(1 - v), \tag{4.3}$$

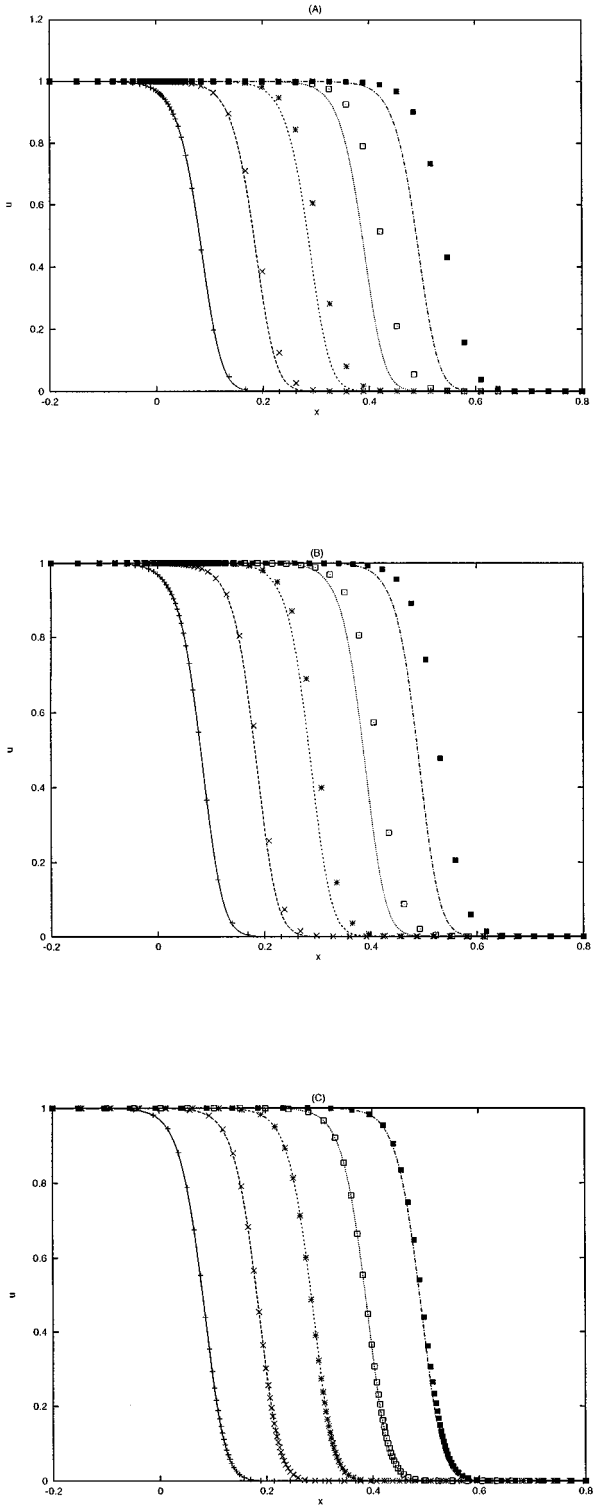

FIG. 6. Numerical solutions of Fisher's equation (1.6) at times $t = 5 \times 10^{-4}$, $t = 1 \times 10^{-3}$, $t = 1.5 \times 10^{-3}$, $t = 2 \times 10^{-3}$ and $t = 2.5 \times 10^{-3}$, computed by MMPDE6 and the modified monitor function (3.5): (a) solution with $\tau = 10^{-3}$; (b) solution with $\tau = 10^{-5}$; (c) solution with $\tau = 10^{-7}$.

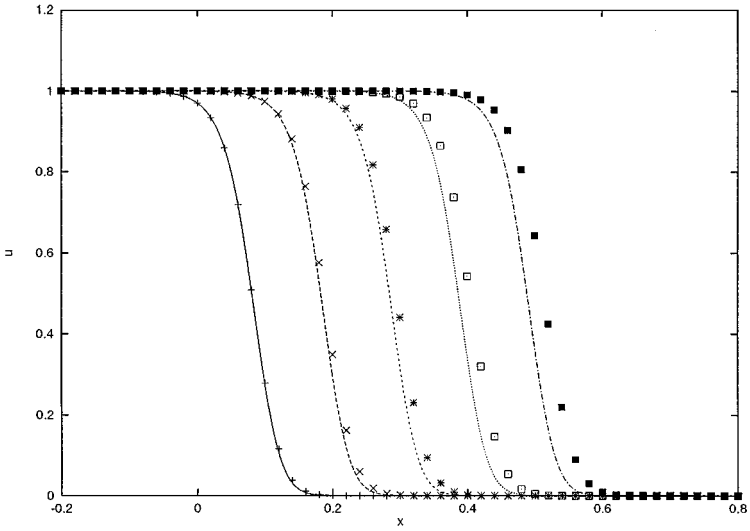

FIG. 7. Numerical solutions of Fisher's equation (1.6) at times $t = 5 \times 10^{-4}$, $t = 1 \times 10^{-3}$, $t = 1.5 \times 10^{-3}$, $t = 2 \times 10^{-3}$, and $t = 2.5 \times 10^{-3}$, computed by the method of lines on an even mesh with $N = 50$.

with boundary conditions similar to (4.2). A comparison of (4.1) and (4.3) shows that the travelling wave is a steady-state solution of (4.3).

To perform a linear stability analysis we write

$$v(\xi, t) = V(\xi) + \eta(\xi, t), \tag{4.4}$$

where squares of η are sufficiently small to be ignored. The linearisation about V shows that η satisfies

$$\frac{\partial \eta}{\partial t} = \frac{\partial^2 \eta}{\partial \xi^2} + c\frac{\partial \eta}{\partial \xi} + \rho(1 - 2V)\eta, \tag{4.5}$$

and, since we are interested in local perturbations, we impose the boundary conditions

$$\eta(\pm L, t) = 0. \tag{4.6}$$

Here we have used $x_R = -x_L = L$ for convenience. Equation (4.5) is converted to self-adjoint form [3] by means of the transformation $\eta(\xi, t) = \exp(-c\xi/2)\, f(\xi, t)$, and f is a solution of

$$\frac{\partial f}{\partial t} = \frac{\partial^2 f}{\partial \xi^2} + \left(-\frac{c^2}{4} + \rho - 2\rho V\right) f \tag{4.7}$$

satisfying boundary conditions (4.6). Note that as $\xi \to \infty$, η must decay to zero at least as $O(e^{-c\xi})$, so $f = e^{c\xi/2}\eta$ will decay exponentially as $|\xi| \to \infty$.

A phase plane analysis of (4.1) and (4.2) shows that there is a unique travelling wave solution for each value of c satisfying $c \geq 2\sqrt{\rho}$ [10]. Furthermore, the wave profile is given by the solution on the trajectory that connects the saddle point at $V = 1, dV/d\xi = 0$ with the stable node at $V = 0, dV/d\xi = 0$. The travelling waves are identical to travelling wave solutions of the Korteweg–de Vries–Burgers (KdVB) equation when dissipation dominates dispersion. The KdVB equation is Burgers' equation with a dispersive term added in the

form of a third-order spatial derivative; it is found useful, for example, in describing plasma shocks [3, 16].

Noting that $c \geq 2\sqrt{\rho}$ we write (4.7) as

$$\frac{\partial f}{\partial t} = \frac{\partial^2 f}{\partial \xi^2} + \rho(1 - s^2 - 2V)\, f, \tag{4.8}$$

were $s \geq 1$. To examine the stability of a numerical solution we consider an even grid with nodes $\{\xi_j\}_{j=0}^{N+1}$, where $\xi_j = -L + jh$ and $h = 2L/(N+1)$. If $f_j (= f_j(t))$ denotes the approximation at (ξ_j, t) the set of semi-discrete equations is

$$h^2 \dot{f}_j = f_{j-1} - \left[2 - \rho h^2 \left(1 - s^2 - 2V_j\right)\right] f_j + f_{j+1}, \quad j = 1, 2, \ldots N, \tag{4.9}$$

with

$$f_0 = f_{N+1} = 0. \tag{4.10}$$

In the analysis we use a simplified model in which V_j is given by the exact solution (see (1.7)):

$$V_j = \left[1 + \exp\left(\sqrt{\frac{\rho}{6}}\xi_j\right)\right]^{-2}. \tag{4.11}$$

System (4.9)–(4.10) may be written in matrix form as

$$\dot{\mathbf{f}} = A\mathbf{f}, \tag{4.12}$$

where $\mathbf{f} = [\, f_1,\ f_2, \ldots,\ f_N]^{\mathrm{T}}$ and

$$A = \frac{1}{h^2}\,\mathrm{tridiag}\{1, -(2 + q_j), 1\}, \tag{4.13}$$

with

$$q_j = \rho h^2 \left(s^2 + 2V_j - 1\right). \tag{4.14}$$

Since $V_j \in (0, 1)$ and $s^2 \geq 1$ it follows from Gerschgorin's theorem that the eigenvalues of the symmetric matrix A are all real and negative. Hence $\|\mathbf{f}\|$ decays exponentially with time and the system is linearly stable to local disturbances.

Table I shows the eigenvalues, $\{\lambda_k\}_{k=1}^{N}$, of A corresponding to $N = 9$, 19, and 29. In the calculation we have used the values $\rho = 10^4$, $L = \frac{1}{2}$, and $s = 5/2\sqrt{6}$ that correspond to the travelling wave (1.7). The eigenvalues are ordered such that

$$\lambda_N < \lambda_{N-1} < \cdots < \lambda_1 < 0. \tag{4.15}$$

TABLE I

Eigenvalues of Matrix A in (4.12) with $\rho = 10^4$, $s = 5/2\sqrt{6}$, and $L = \frac{1}{2}$

N	λ_N	λ_{N-1}	λ_{N-2}	$\cdots$	λ_3	λ_2	λ_1
9	-2.08×10^4	-2.06×10^4	-2.05×10^4	$\cdots$	-6.80×10^2	-5.56×10^2	-4.55×10^2
19	-2.20×10^4	-2.18×10^4	-2.15×10^4	$\cdots$	-7.71×10^2	-5.82×10^2	-4.59×10^2
29	-2.40×10^4	-2.38×10^4	-2.35×10^4	$\cdots$	-7.89×10^2	-5.86×10^2	-4.60×10^2

If $A\mathbf{x}^{(k)} = \lambda_k \mathbf{x}^{(k)}$, $k = 1, 2, \ldots, N$, then the solution of (4.12) is

$$\mathbf{f}(t) = \sum_{k=1}^{N} c_k \mathbf{x}^{(k)} e^{\lambda_k t}, \tag{4.16}$$

where $\{c_k\}_{k=1}^{N}$ are given by the initial conditions on $\mathbf{f}$.

With an initial perturbation ϵ confined to node x_1, we may write $f_1(0) = \epsilon$ and $f_j(0) = 0$ for $j \neq 1$. The solution (4.16) takes the form

$$\mathbf{f}(t) = \epsilon \sum_{k=1}^{N} x_1^{(k)} \mathbf{x}^{(k)} e^{\lambda_k t}, \tag{4.17}$$

where $\mathbf{x}^{(k)} = [x_1^{(k)}, x_2^{(k)}, \ldots, x_N^{(k)}]^{\mathrm{T}}$ and $\|\mathbf{x}^{(k)}\|_2 = 1$. The computed results show that $x_1^{(k)} \sim 0$ for all k except $k = N, N-1, \ldots, N-n$, where $n \sim O(N/3)$. It follows that the perturbation at x_1 yields a solution that is a sum over the $n+1$ most rapidly decaying exponentials in (4.16). Similarly, a perturbation at x_N yields a solution that is a sum over the $n+1$ most slowly decaying exponentials in (4.16). The rate of decay of a perturbation on nodal values at the back of the wave is thus greater than that for a perturbation on nodal values at the front of the wave. Table I shows that for $\rho = 10^4$, the fastest and slowest decaying modes have decay rates of order $\exp(-2.4 \times 10^4 t)$ and $\exp(-4.6 \times 10^2 t)$, respectively. This seems to suggest that disturbances near x_1 or near x_N will decay with extreme rapidity. However, the time scale of a typical numerical experiment is $t = 2.5 \times 10^{-3}$, and the decay factors over this time scale near x_1 and x_N are, respectively, $\exp(-60)$ and $\exp(-1.15)$. It follows that perturbations at the rear of the wave are insignificant, relative to analogous perturbations at the wave front.

The eigenvalue computations described above were also performed using a discretisation of (4.8) on a grid that was generated adaptively. The grid was formed by adapting to the exact solution $V(\xi)$ of (4.1) and (4.2) by equidistribution of the monitor function (3.5). The adaptive computation yields the same qualitative effects as the uniform grid computation. The convergence of λ_1 to the value -460 (see Table I) is faster in the adaptive case. Also, the value of the ratio λ_N/λ_1 for a particular value of N in the uniform grid case is attained at a much lower value of N in the adaptive case. For example, the value of λ_N/λ_1 in the uniform grid case with $N = 299$ is comparable with the value in the adaptive grid case with $N = 49$.

It is of interest to note how the stability on the finite domain differs from that on the infinite domain. Note, initially, that $dV/d\xi \equiv V_\xi$ is a solution of

$$\mathcal{L}V_\xi = 0, \tag{4.18}$$

where $\mathcal{L}$ denotes the linear differential operator given by the right-hand side of (4.5). Furthermore, V_ξ decays exponentially to zero as $|\xi| \to \infty$ and it follows that $\mathcal{L}$ has a zero eigenvalue for the pure Cauchy problem. A perturbation, ϵV_ξ, that is a multiple of V_ξ will therefore continue to exist with no decay or growth, and since

$$V(\xi + \epsilon) = V(\xi) + \epsilon V_\xi(\xi) + O(\epsilon^2), \tag{4.19}$$

it follows that small perturbations of this type may only result in a phase shift of the original travelling wave. The finite domain problem does not exhibit this property since $V_\xi \neq 0$ at $\xi = \pm L$, but numerical approximations over a large finite domain may be expected to have a tendency to suffer phase errors that arise from perturbations which have a nonzero projection in the space spanned by the discretised representation of V_ξ.

To support this expectation, one should note that if $\mathcal{L}_h$ denotes the second-order central difference approximation to $\mathcal{L}$ and if $(V_\xi)_h$ denotes the vector $\{dV/d\xi(\xi_j)\}_{j=0}^{N+1}$, then the residual $\mathcal{L}_h(V_\xi)_h$ is $O(h^2)$ as $h \to 0$ for a fixed value of L. For sufficiently small h, and sufficiently large L, $(V_\xi)_h$ is a close approximation to an eigenvector of $\mathcal{L}_h$ corresponding to the nearly zero eigenvalue. The tendency of $\mathcal{L}_h(V_\xi)_h$ to zero as $h \to 0$ is readily verified numerically.

The eigenvalues of $\mathcal{L}_h$ were computed at several values of N with $\rho = 1$ and $L = 25$, and it was noted that the eigenvalues are all real and negative if N is sufficiently large. The negative eigenvalue of smallest modulus, μ, is $O(h^2)$ as $h \to 0$. For example, at $N = 159$, $N = 319$, and $N = 639$, the values of μ are -0.0086, -0.0016, and -0.0004, respectively. To confirm the behaviour of the least negative eigenvalue as the discretisation is refined, the operator $\mathcal{L}$ was discretised using a pseudospectral method with nodes at scaled Chebyshev–Gauss–Lobatto points $\xi_j = -L\cos(\pi j/N)$, $j = 0, 1, \ldots, N$; at $N = 70$ we obtain a zero eigenvalue to four decimal digits. Finally, reverting to second-order central differences, the eigenvecter associated with μ at $N = 159$ is shown in Fig. 8a, and the vecter $(V_\xi)_h$ is shown in Fig. 8b.

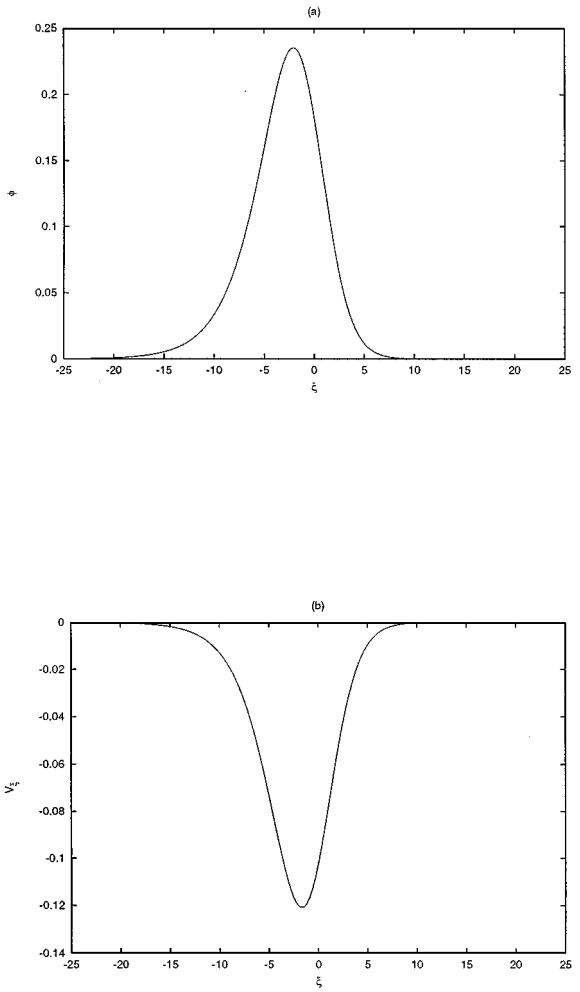

FIG. 8. Tendency of $(V_\xi)_h$ to an eigenvector of $\mathcal{L}_h$ corresponding to the eigenvalue μ, with $\rho = 1$, $L = 25$, and $N = 159$: (a) shows the eigenvector and (b) shows $(V_\xi)_h$.

Note that $(V_\xi)_h$ is approximated by a suitably scaled version of the eigenvector. This confirms that $(V_\xi)_h$ is a close approximation to an eigenvector of $\mathcal{L}_h$ corresponding to the nearly zero eigenvalue.

5. CONCLUDING REMARKS

We have shown that moving mesh methods based on equidistribution of arc-length or curvature are not suitable for simulating the travelling wave solution of Fisher's equation over a reasonably large time interval. It has also been shown that moving mesh methods produce much better results if the monitor function is chosen to suit the properties of the differential equation and of the solution that is being computed. The preceding section has indicated, *inter alia*, that the solution is more sensitive to errors at the wave front than to errors at the back of the wave, and these properties give guidance on the nodal distributions that might be required. Even when the monitor function is constructed with care, the computed solution may be highly inaccurate if the selected moving mesh method is inappropriate. We have shown that a MMPDE that contains a temporal smoothing parameter may be unsuitable if the parameter value is not consistent with the solution being computed. The MMDAE—which attempts to impose equidistribution at each time step—offers a more reliable approach for this strong reaction problem.

The experiments described here indicate that more needs to be done on the formulation and analysis of moving mesh methods for reaction diffusion equations. The combination of moving mesh methods and the boundary conditions of Hagstrom and Keller [11] should be investigated. Here we have used central differences to approximate u_x in the convection term $\dot{x}u_x$. In situations like those arising in Fisher's equation, where the mesh speed is large near the wave, greater care may be needed in approximating this term. Li and Petzold [18] have suggested that high order upwind approximations should be used to approximate this term.

APPENDIX

Here we consider the index of the differential-algebraic system defined by Eqs. (2.4) and (2.11). To simplify the presentation we select the monitor function (3.2), with $\alpha = 1$ and with smoothing omitted. Under these conditions, Eq. (2.11) assumes the simple form

$$(x_{i+1}-x_i)^2+(u_{i+1}-u_i)^2-(x_i-x_{i-1})^2-(u_i-u_{i-1})^2=0, \quad i=1,2,\ldots,N-1. \tag{6.1}$$

The DAE defined by (2.4) and (6.1) is conveniently written as

$$\dot{\mathbf{u}} - G\dot{\mathbf{x}} = \mathbf{F}, \tag{6.2}$$

$$\mathbf{0} = \mathbf{H}, \tag{6.3}$$

where H_i denotes the left-hand side of Eq. (6.1). One differentiation of (6.3) with respect to t leads to the system

$$(\mathbf{H}_\mathbf{x} + \mathbf{H}_\mathbf{u}G)\dot{\mathbf{x}} = -\mathbf{H}_\mathbf{u}\mathbf{F}. \tag{6.4}$$

If $\mathbf{H}_\mathbf{x} + \mathbf{H}_\mathbf{u}G$ is nonsingular near a solution trajectory then (6.4) gives an explicit expression for $\dot{\mathbf{x}}$, and $\dot{\mathbf{u}}$ may then be obtained explicitly from (6.2). It follows that the DAE is an index 1 system if and only if $\mathbf{H}_\mathbf{x} + \mathbf{H}_\mathbf{u}G$ is nonsingular (see [2, 12]).

From (6.1) we obtain

$$\begin{aligned}
\partial H_i/\partial x_{i-1} &= 2(x_i - x_{i-1}) = 2\alpha_{i-1}, \quad \text{say},\\
\partial H_i/\partial x_i &= -2(x_{i+1} - x_{i-1}) = -2(\alpha_{i-1} + \alpha_i),\\
\partial H_i/\partial x_{i+1} &= 2(x_{i+1} - x_i) = 2\alpha_i,\\
\partial H_i/\partial u_{i-1} &= 2(u_i - u_{i-1}) = 2\beta_{i-1}, \quad \text{say},\\
\partial H_i/\partial u_i &= -2(u_{i+1} - u_{i-1}) = -2(\beta_{i-1} + \beta_i),\\
\partial H_i/\partial u_{i+1} &= 2(u_{i+1} - u_i) = 2\beta_i.
\end{aligned} \tag{6.5}$$

If $\{x_i\}_{i=0}^N$ is a strictly monotonic increasing sequence then $\mathbf{H_x}$ is diagonally dominant and therefore nonsingular.

Also, $G = \text{diag}(G_1, G_2, \ldots, G_{N-1})$, where

$$G_i = \frac{u_{i+1} - u_{i-1}}{x_{i+1} - x_{i-1}} = \frac{\beta_{i-1} + \beta_i}{\alpha_{i-1} + \alpha_i}. \tag{6.6}$$

Since $\mathbf{H_x}$ and $\mathbf{H_u}$ are symmetric, it follows that $\mathbf{H_x} + \mathbf{H_u}G$ is nonsingular if and only if $(\mathbf{H_x} + \mathbf{H_u}G)^{\mathrm{T}} = \mathbf{H_x} + G\mathbf{H_u}$ is nonsingular. It is readily seen that

$$[G\mathbf{H_u}]_{i,j} = \begin{cases} -2(\beta_{i-1} + \beta_i)^2/(\alpha_{i-1} + \alpha_i), & j = i,\\ 2\beta_{i-1}(\beta_{i-1} + \beta_i)/(\alpha_{i-1} + \alpha_i), & j = i-1,\\ 2\beta_i(\beta_{i-1} + \beta_i)/(\alpha_{i-1} + \alpha_i), & j = i+1,\\ 0, & |i-j| > 1. \end{cases} \tag{6.7}$$

From (6.5) and (6.7) we obtain

$$[\mathbf{H_x} + G\mathbf{H_u}]_{i,j} = \begin{cases} -2(\alpha_{i-1} + \alpha_i) - 2(\beta_{i-1} + \beta_i)^2/(\alpha_{i-1} + \alpha_i), & j = i,\\ 2\alpha_{i-1} + 2\beta_{i-1}(\beta_{i-1} + \beta_i)/(\alpha_{i-1} + \alpha_i), & j = i-1,\\ 2\alpha_i + 2\beta_i(\beta_{i-1} + \beta_i)/(\alpha_{i-1} + \alpha_i), & j = i+1,\\ 0, & |i-j| > 1. \end{cases} \tag{6.8}$$

If $R := S(\mathbf{H_x} + G\mathbf{H_u})$, where

$$S = \frac{1}{2}\text{diag}(\alpha_0 + \alpha_1, \alpha_1 + \alpha_2, \ldots, \alpha_{N-2} + \alpha_{N-1}),$$

then S is nonsingular, provided $\{x_i\}_{i=0}^N$ is a strictly monotonic increasing sequence. Under this assumption, it is sufficient to show that R is nonsingular. The elements in row i of R are given by

$$[R]_{i,i} = -(x_{i+1} - x_{i-1})^2 - (u_{i+1} - u_{i-1})^2, \tag{6.9}$$

$$[R]_{i,i-1} = (x_i - x_{i-1})(x_{i+1} - x_{i-1}) + (u_i - u_{i-1})(u_{i+1} - u_{i-1}), \tag{6.10}$$

$$[R]_{i,i+1} = (x_{i+1} - x_i)(x_{i+1} - x_{i-1}) + (u_{i+1} - u_i)(u_{i+1} - u_{i-1}). \tag{6.11}$$

It is convenient to define $[R]_{i,i}$, $[R]_{i,i-1}$ and $[R]_{i,i+1}$ by (6.9)–(6.11) for all $i = 1, 2, \ldots, N-1$. We now show that R is diagonally dominant. Four cases are considered:

(a) $R_{i,i-1} \geq 0$ and $R_{i,i+1} \geq 0$ for any $i = 1, 2, \ldots, N-1$. For this value of i, $|R_{i,i}| = R_{i,i-1} + R_{i,i+1}$.

(b) $R_{i,i-1} < 0$ and $R_{i,i+1} < 0$ for any $i = 1, 2, \ldots, N-1$. Here,

$$|R_{i,i-1}| + |R_{i,i+1}| = -(x_{i+1} - x_{i-1})^2 - (u_{i+1} - u_{i-1})^2 < 0, \tag{6.12}$$

which is a contradiction, so this case does not arise.

(c) $R_{i,i-1} < 0$ and $R_{i,i+1} \geq 0$ for any $i = 1, 2, \ldots, N-1$. In this case,

$$\begin{aligned} |R_{i,i-1}| + R_{i,i+1} &= -(x_i - x_{i-1})(x_{i+1} - x_{i-1}) - (u_i - u_{i-1})(u_{i+1} - u_{i-1}) \\ &\quad + (x_{i+1} - x_i)(x_{i+1} - x_{i-1}) + (u_{i+1} - u_i)(u_{i+1} - u_{i-1}) \\ &= -(x_i - x_{i-1})^2 - (u_i - u_{i-1})^2 + (x_{i+1} - x_i)^2 + (u_{i+1} - u_i)^2 \\ &= 0, \quad \text{using (6.3)}. \end{aligned}$$

(d) $R_{i,i-1} \geq 0$ and $R_{i,i+1} < 0$ for any $i = 1, 2, \ldots, N-1$. This case is analogous to case (c).

It follows from (a)–(d) that

$$|R_{i,i}| \geq |R_{i,i-1}| + |R_{i,i+1}| \quad \text{for all } i = 1, 2, \ldots, N-1, \tag{6.13}$$

and this establishes that $R = S(\mathbf{H_x} + G\mathbf{H_u})$ is diagonally dominant and, thus, nonsingular. Hence, $\mathbf{H_x} + \mathbf{H_u}G$ is nonsingular, and the DAE (6.2)–(6.3) is an index 1 system.

REFERENCES

1. J. G. Blom, J. M. Sanz-Serna, and J. G. Verwer, On simple moving grid methods for one-dimensional evolutionary partial differential equations, *J. Comput. Phys.* **74**, 191 (1988).
2. K. E. Brenan, S. L. Campbell, and L. R. Petzold, *Numerical Solution of Initial-Value Problems in Differential-Algebraic Equations* (Elsevier, Amsterdam, 1989).
3. J. Canosa, On a nonlinear diffusion equation describing population growth, *IBM J. Res. Develop.* **17**, 307 (1973).
4. G. F. Carey and H. T. Dinh, Grading functions and mesh redistribution, *SIAM J. Numer. Anal.* **22**, 1028 (1985).
5. J. M. Coyle, J. E. Flaherty, and R. Ludwig, On the stability of mesh equidistribution strategies for time-dependent partial differential equations, *J. Comput. Phys.* **62**, 26 (1986).
6. E. A. Dorfi and L. O'C. Drury, Simple adaptive grids for 1-D initial value problems, *J. Comput. Phys.* **69**, 175 (1987).
7. R. A. Fisher, The wave of advance of advantageous genes, *Ann. Eugenics* **7**, 355 (1937).
8. J. Gazdag and J. Canosa, Numerical solution of Fisher's equation, *J. Appl. Probab.* **11**, 445 (1974).
9. P. Grinrod, *Patterns and Waves in Reaction-Diffusion* (Oxford Univ. Press, London, 1991).
10. P. S. Hagan, Traveling wave and multiple wave solutions of parabolic equations, *SIAM J. Math. Anal.* **13**, 717 (1982).
11. T. Hagstrom and H. B. Keller, The numerical calculation of traveling wave solutions of non-linear parabolic equations, *SIAM J. Sci. Stat. Comput.* **7**, 978 (1986).
12. E. Hairer and G. Wanner, *Solving Ordinary Differential Equations II: Stiff and Differential-Algebraic Problems*, 2nd ed. (Springer-Verlag, Berlin, 1996).
13. W. Huang, Y. Ren, and R. D. Russell, Moving mesh partial differential equations (MMPDEs) based on the equidistribution principle, *SIAM J. Numer. Anal.* **31**, 709 (1994).
14. W. Huang, Y. Ren, and R. D. Russell, Moving mesh methods based on moving mesh partial differential equations, *J. Comput. Phys.* **113**, 279 (1994).

15. W. Huang and R. D. Russell, *Moving Mesh Strategy Based upon a Heat Flow Equation for Two-Dimensional Problems*, Kansas Univ. Math. Res. Rep. 96-04-03 (1996).
16. A. Jeffrey and T. Kakutani, Weak nonlinear despersive waves: A discussion centred around the KdV equation, *SIAM Rev.* **14**, 582 (1972).
17. A. Kolmogorov, I. Petrovsky, and N. Piscounoff, Étude de l'équation de la diffusion avec croissance de la quantité de matière et son application à un problème biologique, *Bull. Univ. Etat Moscou (Ser. Int.)* **A1**, 1 (1937).
18. S. Li and L. R. Petzold, Moving mesh methods with upwinding schemes for time-dependent PDEs, *J. Comput. Phys.* **131**, 368 (1997).
19. S. Li, L. R. Petzold, and Y. Ren, Stability of moving mesh system of partial differential equations, *SIAM J. Sci. Comput.*, submitted.
20. L. S. Mulholland, Y. Qiu, and D. M. Sloan, Solution of evolutionary partial differential equations using adaptive finite differences with pseudospectral post-processing, *J. Comput. Phys.* **131**, 280 (1997).
21. L. R. Petzold, *A Description of DASSL: A Differential/Algebraic System Solver*, SAND 82-8637, Sandia Labs, Livermore, CA, 1982.
22. Y. Qiu and D. M. Sloan, *On Multiple Solutions of a Convection-Diffusion Boundary Value Problem Produced by an Adaptive Mesh Method*, Strathclyde Univ. Math. Res. Rep. 42 (1997).
23. M. A. Revilla, Simple time and space adaptation in one-dimensional evolutionary partial differential equations, *Int. J. Num. Meth. Eng.* **23**, 2263 (1986).